

# **Whole transcriptome analysis by RNA-Seq, a state-of-the-art technique to uncover complex biological processes. The blackberry example.**

**Perez-Aso, Miguel<sup>1\*</sup>; Rubio, Emilio<sup>1</sup>; Reina, Manuel<sup>2</sup>; Müller-Sánchez, Claudia<sup>2</sup>; Bosch, Jordi<sup>1</sup>**

<sup>1</sup> Provital S.A.U., Barcelona, Spain

<sup>2</sup> Department of Cell Biology, Physiology and Immunology, Celltec-UB, University of Barcelona, Barcelona, Spain

\* Perez-Aso, Miguel, (+34) 93 719 23 50, [m.aso@weareprovital.com](mailto:m.aso@weareprovital.com).

## **Abstract**

### **Background:**

Although it is well-known that the blackberry is linked to various health benefits, little is known about its impact on adipocyte biology. Therefore, in the present work we sought to analyze the impact of a blackberry extract (*Rubus fruticosus* fruit extract, RFE) on adipogenesis and lipolysis in the 3T3-L1 cell model, followed by a comprehensive transcriptomic analysis.

### **Methods:**

The impact of RFE on adipogenesis and lipolysis in 3T3-L1 differentiated adipocytes was analyzed by Oil Red O and AdipoRed™ staining and glycerol measurement, respectively. To follow, the transcriptome was sequenced by RNA-Seq and data was subsequently processed with the PIGx bioinformatic pipeline and differential expression statistical analysis was performed using edgeR.

### **Results:**

RFE elicits a strong adipogenic effect, as shown by an increase of 29 % (n=3, P<0.01) in Red Oil O staining, as well as anti-lipolytic activity, detected by a decrease of 51 % (n=3, P<0.05) on glycerol release. Whole transcriptomic analysis by RNA-Seq showed that RFE

significantly regulates the expression of 4904 genes and enhances the adipogenic program. Functional profiling revealed metabolic pathways modified by RFE, as well as unexpected routes modulated by RFE. Of particular interest was the finding that pathways regulating the adipose extracellular matrix (ECM) were also regulated by RFE.

### **Conclusion:**

The present work represents, to the best of our knowledge, the first direct evidence that RFE facilitates adipocyte differentiation as a whole, including the ECM remodeling required for a healthy adipocyte maturation, as revealed by a comprehensive transcriptomic analysis.

**Keywords:** *Rubus fruticosus*, transcriptomics, RNA-Seq, adipogenesis, lipolysis

### **Introduction.**

At the dawn of the transcriptomic era in cosmetic science, we are beginning to understand its potential. The transcriptome, the total amount of RNA transcribed by specific cells and tissues in an organism at specific physiological condition, can be analyzed by several technologies, among which RNA sequencing (RNA-Seq) has obvious advantages, such as good repeatability, high sensitivity, and wide detection range. Therefore, RNA-Seq has gradually replaced other technologies and is widely used for transcriptomic analysis [1]. However, RNA-Seq faces several bioinformatic challenges, including computational analyses of big data, a cumbersome task.

It is well known that the blackberry is linked to various health benefits, e.g. the prevention and treatment of metabolic syndrome, support of the digestive and immune system, prevention of inflammatory disorders, cardiovascular diseases and protective effects against gastrointestinal tract cancers [2]. The blackberry is also used in cosmetics, mainly due to its antioxidant and anti-inflammatory properties, making it suitable for skin antiaging and hair protection applications [3]. However, to our knowledge, currently there is no comprehensive description of the impact of the blackberry in fat accumulation, lipolysis or adipocyte differentiation. Nonetheless, some characteristic phytochemicals of the blackberry, e.g. cyanidin 3-glucoside, ellagitannins and flavonols, have been reported to exert activities on

adipocytes or adipogenic-related processes [4–6]. Therefore, in the present work we sought to study the effect of the blackberry on adipogenesis and adipocyte metabolism by measuring lipid content in the adipocyte, by both Red Oil O and Adipored<sup>TM</sup> staining, lipolysis by glycerol measurement, and by exploring gene expression patterns by RNA-Seq.

To our knowledge, the present study represents, for the first time, that the blackberry (*Rubus fruticosus* fruit extract, RFE) elicits both pro-adipogenic and anti-lipolytic activities in adipocytes. The analysis of the transcriptomic program during preadipocyte differentiation to mature adipocytes stimulated with RFE, revealed mechanisms and functional pathways which help to better understand RFE's impact on adipocytes metabolism.

## Methods.

### Tested product

The product assessed in the *in vitro* assays was a concentrated dry extract from the ripe fruits of *Rubus fruticosus* (RFE), which corresponded to its phenolic fraction.

### Cell viability assay

5000 cells were plated in 96-well plates and grown for 24 h. Then, stimulation was performed during 24 h at the indicated concentrations. Thereafter, 10 µl of alamarBlue<sup>TM</sup> cell viability assay reagent (Thermo Scientific, Wilmington, DE) was added and incubated at 37 °C for 2 hours. Absorbance at a wavelength of 570 nm and 600 nm was measured. The reduction of alamarBlue<sup>TM</sup> reagent was calculated following manufacturer's instruction. Cell viability was shown in relative to non-stimulated control.

### 3T3-L1 preadipocyte culture, differentiation and stimulation

3T3-L1 preadipocytes (ATCC, USA. Ref # CL-173) were maintained in DMEM 4.5 g/L glucose medium (Gibco, Carlsbad, CA, USA) supplemented with 10% (v/v) Newborn Calf serum (NCS; Gibco, Carlsbad, CA, USA), 4 mM Glutamine (Gibco, Carlsbad, CA, USA), 25 mM HEPES and 100 µg/ml penicillin/streptomycin (Gibco, Carlsbad, CA, USA) at 37 °C in a humidified atmosphere of 5% CO<sub>2</sub>. For differentiation into adipocytes, as depicted in Figure 2, 3T3-L1 preadipocytes were grown to confluence and overgrow for 48 h. Then,

growth medium was replaced by differentiating medium 1 (DM1; DMEM:F12, Penicillin/streptomycin (110U/ml / 100µl) 1%, FBS 10%, IBMX 0.5mM, Dexamethasone 1µM, Insulin 10 µM, Rosiglitazone 2 µM). After 48 h, DM1 was replaced by differentiating medium 2 (DM2; DMEM:F12, Penicillin/streptomycin (110U/ml / 100µl) 1%, FBS 10%, Insulin 10 µM). For lipid staining, stimulation with RFE was performed at the same time as when growth medium was replaced by DM1, and was repeated when DM1 was replaced by DM2. After 48 h, Oil Red O staining was performed as described below. For lipolysis determination, cells were stimulated with RFE only 24 h after DM1 was replaced by DM2, and glycerol measurement was performed after another 24 h period.

#### *Oil Red O quantification*

To visualize and quantify lipid accumulation, Oil Red O staining was performed using oil Red O solution (Sigma-Aldrich, St. Louis, MO, USA) according to the manufacturer's instructions. Briefly, differentiated adipocytes were fixed in 4% paraformaldehyde for 30 min and washed twice with distilled water. After fixation, wells were incubated with 60% isopropanol for 5 min and dried completely. Finally, freshly Oil Red O Working Solution (3 parts of Oil Red O Stock Solution to 2 parts of water) was added for 10 min and washed 5 times with distilled water. Lipid droplet (LD) was visualized by Zeiss Axiovert phase-contrast microscopy (Carl Zeiss Microscopy GmbH Jena, Thüringen, Germany) at a magnification of 40 ×. After eluting stained LDs with 100% isopropanol, the intracellular lipid content was quantified by measuring the absorbance at 500 nm.

#### *Confocal Microscopy*

To visualize LDs by fluorescence, AdipoRed™ Assay Reagent (Lonza; Basel, Switzerland) was performed according to the manufacturer's instructions. Cells were fixed in 4% paraformaldehyde for 30 min and 5 µL/mL AdipoRed™ reagent was added at the last 10 min of fixation in dark. Subsequently, cells were washed twice with PBS and the nuclei were labelled with Hoechst (Invitrogen; Paisley, Scotland, UK). Stained LDs were visualized and acquired using a LSM 880 confocal laser scanning microscope (Carl Zeiss Microscopy GmbH Jena, Thüringen, Germany).

### Glycerol

To determine the amount of glycerol, supernatants were assayed with Lipolysis colorimetric Assay Kit (Sigma-Aldrich, St. Louis, MO, USA) according to the manufacturer's instructions. Supernatants were mixed with assay reaction mix (1:2) on a 96 well plate and incubated for 20 minutes at RT in dark. A standard curve was made using glycerol standard supplied with concentrations ranging from 0 to 2 mg/mL. The optical density was read at 570 nm on the Infinite 200 PRO multimode reader (Tecan group Ltd. Männedorf, Switzerland). Glycerol was normalized by total protein levels, quantified using Pierce BCA Protein Assay Kit (Thermo Fisher Scientific, Pittsburgh, PA, USA).

### RNA extraction, sequencing and bioinformatic analysis

3T3-L1 preadipocytes were grown, differentiated, and stimulated in triplicates following the protocol described above for lipid determination. Then, RNA from non-differentiated preadipocytes, differentiated adipocytes stimulated and non-stimulated with RFE 0.0625mg/ml, was isolated with the Tripure Isolation Reagent (Roche Diagnostics, Indianapolis, IN, USA) followed by purification with the RNeasy MinElute Cleanup Kit (Qiagen Valencia, CA, USA). RNA quantity and quality was determined by fluorimetry with Qubit (Invitrogen, Carlsbad, CA, USA) and RNA integrity was determined by microfluidic electrophoresis with the Bioanalyzer 2100 (Agilent Technologies, Waldbronn, Germany). Then, 1 ng was used from each sample to construct RNASeq libraries with the Illumina TruSeq RNA v2 library prep kit (Illumina Inc, San Diego, CA, USA). Library QC was carried out with Agilent bioanalyzer DNA1000 and Agilent bioanalyzer HS kits. The libraries were then quantitated with Qubit and pooled in equimolar amounts. Sequencing was carried out in Illumina NovaSeq SP reagent cartridge, producing approximately 25M, Single End, 101 bp long reads for each sample.

Data was analysed with the PIGx pipeline, a workflow that reliably produces consistent results, in terms of reproducibility and traceability [7]. First, raw reads were trimmed using TrimGalore!, a script that automates quality and adapter trimming as well as quality control, so that minimum read quality is assured as well as the outputs. Next, reads were accurately aligned to a reference genome using STAR [8], and depth of coverage was computed using

BEDTools. Gene level expression counts were obtained from STAR. Low-expressed genes were filtered according to the Jaccard Similarity Index criteria [9] implemented in the HTSfilter R package [10]. Next, the function TopTags of the R package edgeR [11] was used to create a table of Differentially Expressed Gene (DEG) list. Functional Analysis was then performed with the R package gprofiler2 [12, 13] using the 1000 topmost DEGs. Graphical representation of significantly enriched terms was performed with the over-representation analysis (ORA) function (g:GOSt) of the gprofiler2 R package [12, 13].

#### Statistical analysis

Results are presented as the mean  $\pm$  S.E.M. for n experiments. A statistical analysis was performed by the two-way One Way ANOVA followed by Tukey's post- test using Prism version 9 (Graphpad Software, La Jolla, CA, USA). Significance was defined as P<0.05. In the differential expression analysis of the transcriptomics study, the statistical analysis was calculated with the function decideTestDGE of the edgeR software, where a FDR value < 0.05 was considered significant. For the functional enrichment analysis with the gprofiler2 R package, a p value threshold of 0.05 was selected.

## **Results.**

### RFE shows no cytotoxic effect.

We first tested whether RFE showed any cytotoxic effect by incubating 3T3-L1 preadipocytes with increasing concentrations of RFE, ranging from 0.00390625 to 0.25 mg/ml. The cell viability assay was performed as described in the *Methods* section. As shown in Figure 1, there was no cytotoxicity registered at any of the concentrations tested.

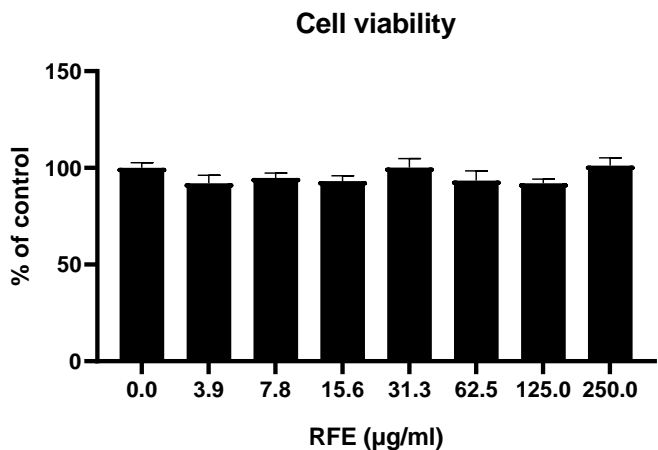
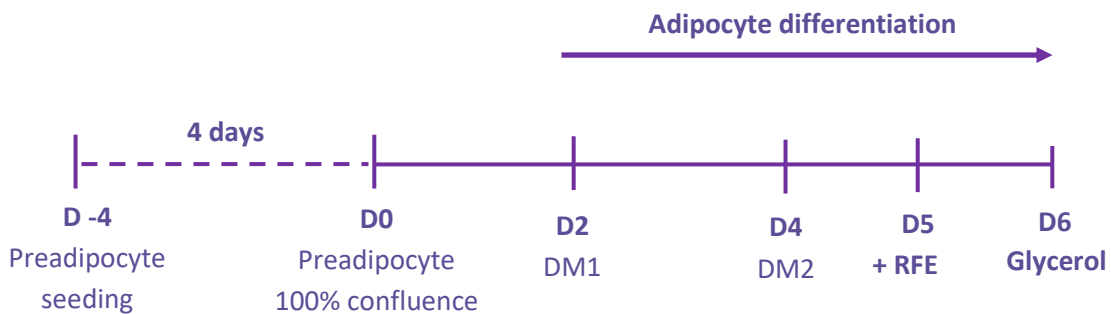


**Figure 1.** RFE is not cytotoxic on 3T3-L1 preadipocytes at any of the concentrations. Data represent mean  $\pm$  SEM.

RFE reduces lipolysis and increases lipogenesis in mature adipocytes

We next studied the impact of RFE in lipid accumulation and degradation in 3T3-L1 differentiated adipocytes. To do so, as fully described above under *Methods*, we followed the differentiation protocol depicted in Figure 2A for the determination of lipid breakdown (lipolysis) by glycerol measurement, while the protocol depicted in Figure 2B was performed to analyse lipid accumulation (lipogenesis) by Oil Red O lipid staining. As negative control for both assays, the same measurements were performed on 3T3-L1 preadipocytes harvested at day 0 (D0) which did not undergo differentiation.

A)



B)

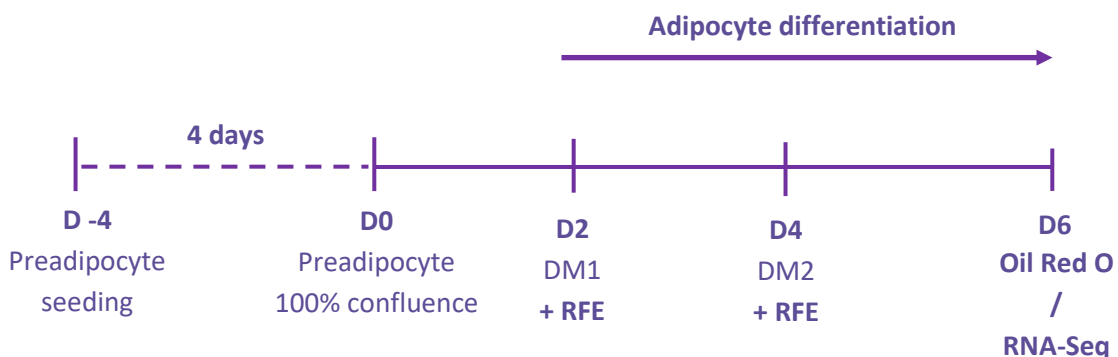


**Figure 2.** Schematic representation of the adipocyte differentiation protocol followed in the present work. Protocol A) was used for measuring lipolysis by glycerol determination and protocol B) was used for measuring adipogenesis by Oil Red O determination or for RNA sequencing (RNA-Seq). The exact composition of DM1 (Differentiation Medium 1) and DM2 (Differentiation Medium 2) is detailed in the *Methods* section.

As shown in Figure 3A, differentiation of preadipocytes into mature adipocytes significantly increased glycerol release, while the treatment with RFE 0.0625 mg/ml of differentiated adipocytes significantly reduced glycerol levels by 51 % ( $n=3$ ,  $P<0.05$ ), indicating that RFE strongly reduces lipolysis in the adipocyte. On the contrary, while Figure 3B shows that adipocyte differentiation increased lipid accumulation, quantified by Red Oil O dye extraction, it was further increased up to 29 % of adipocyte control ( $n=3$ ,  $P<0.01$ ) by RFE 0.0625 mg/ml stimulation, suggesting that RFE facilitates adipogenesis.

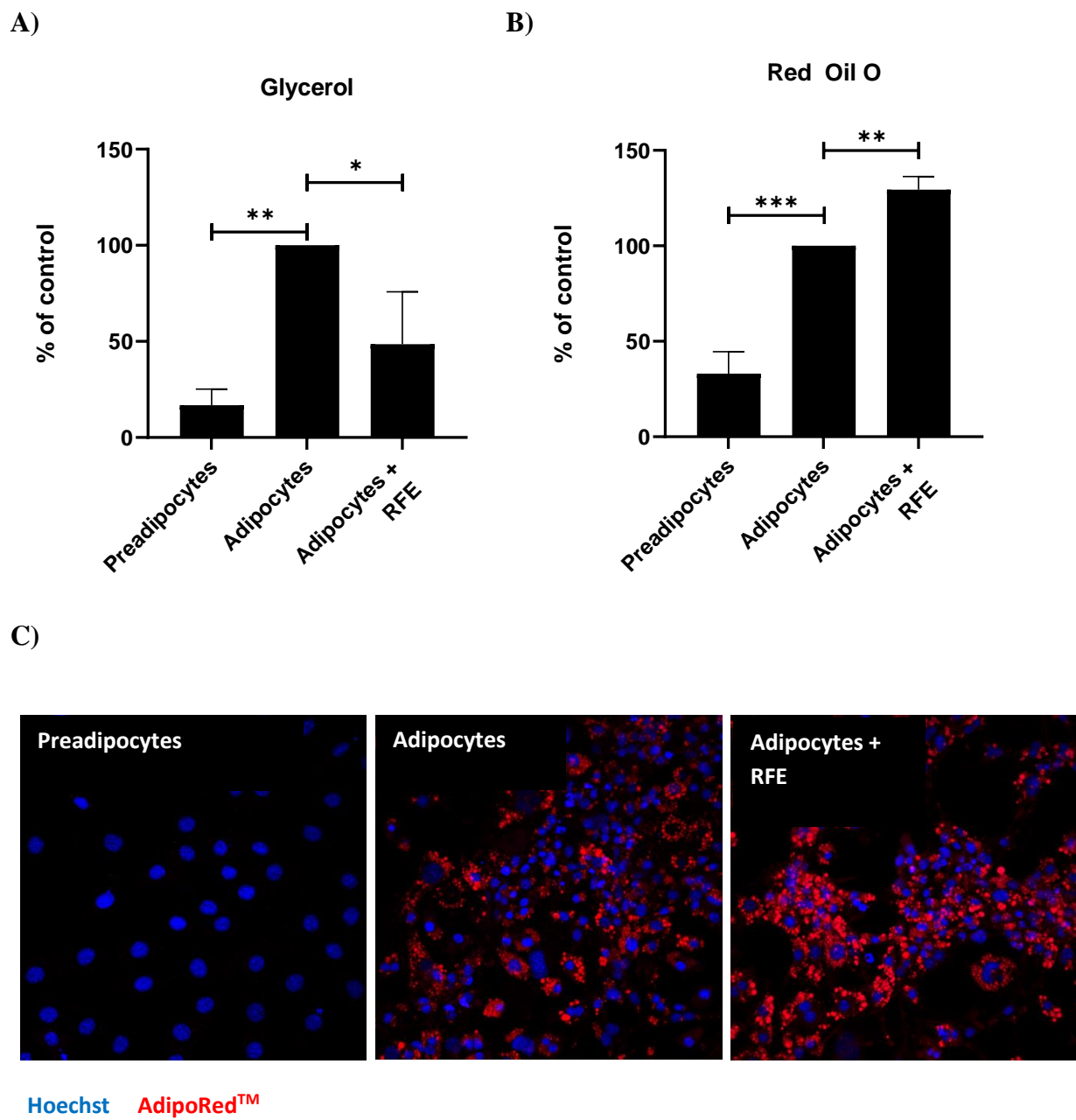


**Figure 3.** RFE impact on lipolysis and adipogenesis. 3T3-L1 preadipocytes, differentiated adipocytes and differentiated adipocytes stimulated with RFE 0.0625 mg/ml were used to analyze **A)** lipolysis by glycerol determination and lipogenesis by **B)** Red Oil O measurement or by **C)** fluorescence imaging with AdipoRed™ staining and Hoechst nuclei labeling. Data represent mean  $\pm$  SEM of three independent experiments. Statistics was performed by One Way ANOVA followed by Tukey's post- test were \*  $P<0.05$ , \*\*  $P<0.01$ , \*\*\*  $P<0.001$  vs. Adipocytes.

To further assess the impact of RFE in lipid accumulation, we next stained lipids with the AdipoRed<sup>TM</sup> reagent, which emits fluorescence allowing therefore its visualization by confocal microscopy. Representative confocal images in Figure 3C illustrate the increase on lipid content elicited by adipocyte differentiation and the facilitation of lipid accumulation by RFE, which further increases AdipoRed<sup>TM</sup> staining when compared to mature adipocytes.

#### RNA sequencing

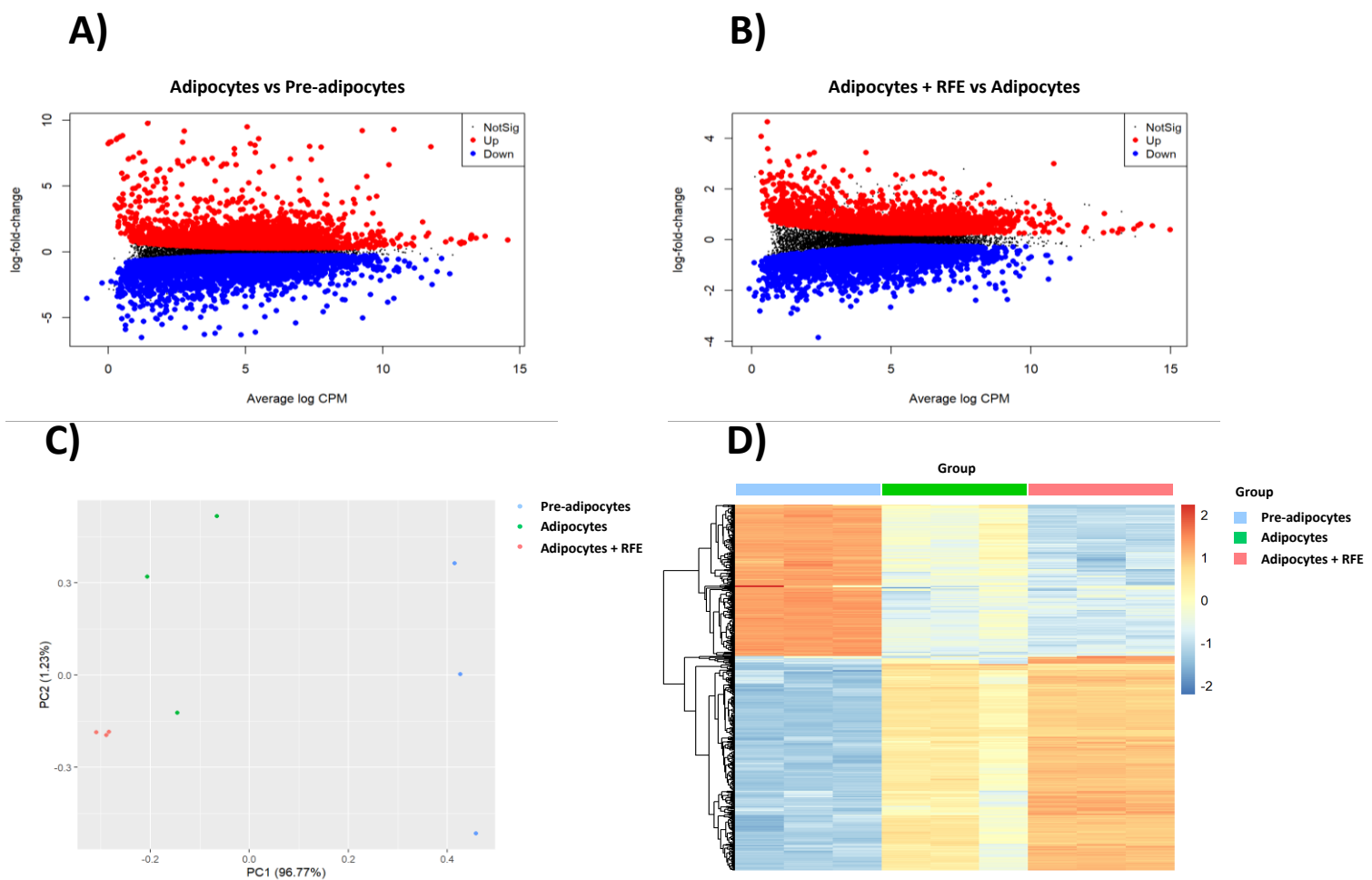
In order to further explore the impact of RFE on the adipocyte, and given the results found in the experiments described above, RNA from adipocytes undergoing differentiation and stimulated with RFE 0.0625 mg/ml was isolated and sequenced by RNA-Seq. As control, RNA from adipocytes and preadipocytes non-stimulated with RFE was also isolated and sequenced.

22 Mb of reads were generated in average for each sample, with a read mean quality > 35 for all samples. Filtered reads were mapped to the reference genome with a mapping rate > 83%. Three conditions were tested in triplicate: Non-Differentiated preadipocytes (Preadipocytes), differentiated adipocytes (Adipocytes) and differentiated adipocytes treated with RFE 0.0625 mg/ml (Adipocytes + RFE). As depicted in the mean-difference plot (MD Plot) on Figure 4A, we detected 3728 genes significantly up-regulated by differentiation (red dots), while 3236 genes were downregulated (blue dots). On the other hand, RFE stimulation of differentiating adipocytes induced a significant upregulation of 2308 genes and significantly downregulated 2596 genes (Figure 4B) when compared to non-treated adipocytes that underwent differentiation.

PCA analysis of all 9 samples (Figure 4C), i.e. three conditions in triplicate, shows clustering along the PC1 axis (96.77 % of gene variance) presenting a clear separation between preadipocytes and differentiated adipocytes. Interestingly, treatment of adipocytes with RFE moved samples over along the PC1 axis and also induced clustering of samples along the PC2 axis (1.23 % gene variance), strongly suggesting that RFE facilitates adipocyte differentiation.

In order to further analyse the gene expression patterns, the heatmap displayed in Figure 4D was generated, showing the clustering of the three different conditions, in triplicate, according to the expression pattern of the 500 topmost variable genes, and it reveals a differentially-expressed gene signature between adipocytes and preadipocytes. Interestingly, visual inspection of the heatmap also shows that stimulation of adipocytes with RPE 0.0625 mg/ml further induces gene expression modifications in the same direction as adipocyte differentiation, i.e. increased genes during adipocyte differentiation are further increased by RFE and the same holds true for inhibited genes, suggesting that RFE facilitates the progression of the pro-adipogenic program.

Taken together, our data serves to better delineate the gene expression signature of adipocyte differentiation, and also strongly suggests that RFE regulates the gene signature of adipogenesis facilitating therefore the progression from preadipocyte to adipocyte.

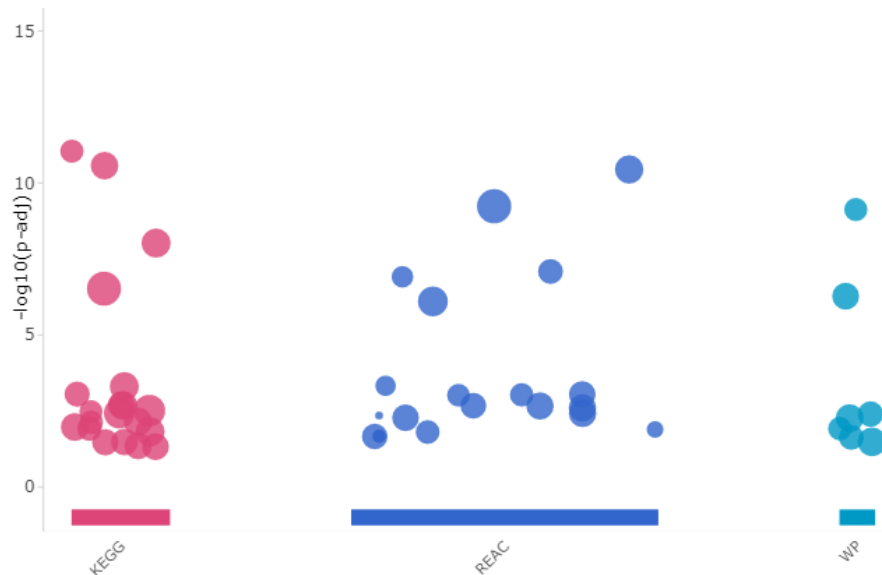


**Figure 4. Differentially Expressed Gene (DEG) profiling.** Mean Difference plot (MD plot) shows Differentially Expressed Genes (DEGs). Non-significant DEGs are depicted in solid black, significant upregulated DEGs are depicted un red and downregulated DEGs in blue when comparing **A**) adipocytes to preadipocytes or **B**) adipocytes stimulated with RFE 0.0625 mg/ml to non-stimulated adipocytes. P-values were calculated using R-package edgeR as described in the *Methods* section. **C**) Principal Component Analysis (PCA) plot. **D**) Heatmap representing gene expression patterns of the 500 topmost variable genes.

#### Functional analysis of DEGs

To better understand the implications of the gene expression patterns described above, we next performed a functional analysis of the 1000 topmost differentially expressed genes. We ran the functional analysis with the databases Kyoto Encyclopedia of Genes and Genomes (KEGG), Reactome (REAC) and WikiPathways (WP) using the gprofiler2 R package [12, 13].

Regarding the adipogenic program, i.e. comparison of adipocytes to preadipocytes, as shown in Figure 5A, a total of 47 pathways were significantly ( $P<0.05$ ) enriched during adipocyte differentiation, when combining the results of all 3 analysed databases. When DEGs were searched against the KEGG database, most enriched pathways were related to metabolism, such as *Metabolic pathways* ( $P=2.99\times 10^{-7}$ ), as was expected since cellular metabolism suffers a dramatic shift from preadipocytes to full-functional adipocytes. Similarly, the central metabolic regulator *Citrate cycle (TCA cycle)* ( $P=8.92\times 10^{-12}$ ) was also significantly enriched. In the same line, the *Citric acid cycle (TCA cycle)* ( $P=3.56\times 10^{-11}$ ) and *Metabolism* ( $P=5.98\times 10^{-10}$ ) were the most enriched and significant pathways when analysing the REAC database. Interestingly, *Extracellular Matrix organization* ( $P=7.83\times 10^{-7}$ ) was also found to be significantly regulated during adipocyte differentiation, according to the REAC database. WP showed *TCA cycle* ( $P=7.42\times 10^{-10}$ ) among the most enriched terms, but also *Adipogenesis genes* ( $P=0.0054$ ), as expected from previous results.

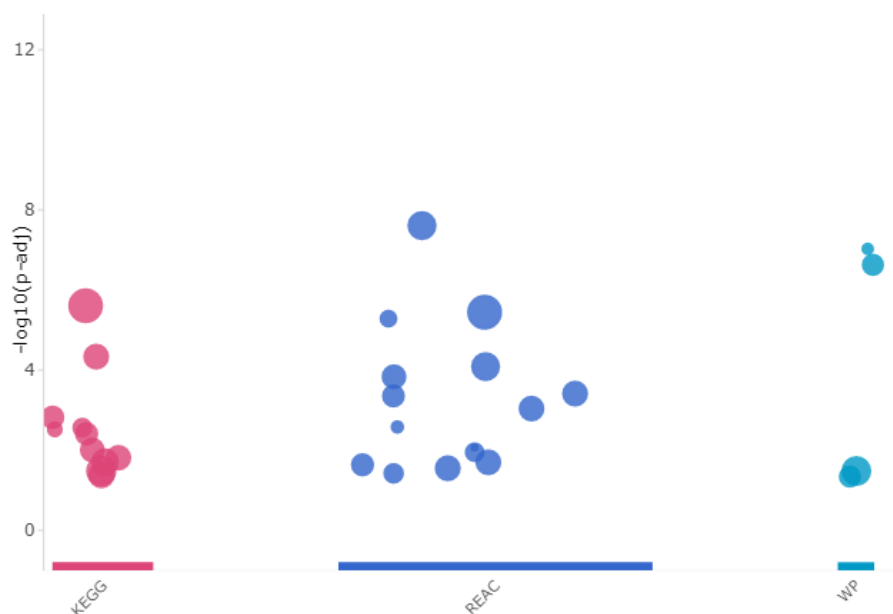
**A)****B)**

KEGG		REAC		WP	
Term	P value	Term	P value	Term	P value
Citrate cycle (TCA cycle)	8.923 e-12	The citric acid (TCA) cycle and respiratory electron transport	3.564 e-11	TCA Cycle	7.421 e-10
Carbon metabolism	2.679 e-11	Metabolism	5.797 e-10	Amino Acid metabolism	5.275 e-7
Diabetic cardiomyopathy	9.443e-9	Pyruvate metabolism and Citric Acid (TCA) cycle	8.115 e-8	Endochondral Ossification	0.0040
Metabolic pathways	2.986e-7	Citric acid cycle (TCA cycle)	1.216 e-7	Adipogenesis genes	0.0054
Focal adhesion	0.0005	Extracellular matrix organization	7.832 e-7	Fatty Acid Beta Oxidation	0.0120
Valine, leucine and isoleucine degradation	0.0009	Branched-chain amino acid catabolism	0.0005	Glycolysis and Gluconeogenesis	0.0233
Cardiac muscle contraction	0.0019	Respiratory electron transport	0.0009	Focal Adhesion	0.0326
Axon guidance	0.0021	O-glycosylation of TSR domain-containing proteins	0.0009		
Glyoxylate and dicarboxylate metabolism	0.0033	Glyoxylate metabolism and glycine degradation	0.0010		
PI3K-Akt signaling pathway	0.0037	Integrin cell surface interactions	0.0021		

**Figure 5. Pathway enrichment analysis of Adipocyte vs. Preadipocyte DEGs.** **A)** Manhattan plot of significantly enriched terms from the DEGs between Adipocyte and Preadipocyte. Databases used were Kyoto Encyclopedia of Genes and Genomes (KEGG), Reactome (REAC) and WikiPathways (WP). **B)** Table showing the top 10 most regulated terms of each database.

Next, we performed a functional analysis with the DEGs regulated by RFE incubation of differentiated adipocytes. As depicted in Figure 6A, 30 pathways were found significantly ( $P<0.05$ ) enriched. The most significantly enriched pathway according to the KEGG

database, as seen in Figure 6B, is *Metabolic pathways* ( $P=2.47 \times 10^{-6}$ ) again suggesting that RFE induces similar enriched functional terms to that of adipocyte differentiation. In agreement with the abovementioned notion that RFE facilitates the adipogenic program, important pathways related to adipocyte differentiation were detected, such as *PPAR signalling pathway* ( $P=0.0099$ , KEGG). Additional support for the role of RFE in inducing the adipogenic program is provided by the finding that RFE stimulation of adipocytes also enriched several pathways involving lipid synthesis. This is the case of the *Biosynthesis of unsaturated fatty acids* ( $P=0.0027$ , KEGG), *Fatty acid metabolism* ( $P=0.0039$ , KEGG), as well as *Cholesterol biosynthesis* ( $P=5.18 \times 10^{-6}$ , REAC), ( $P=9.4 \times 10^{-8}$ , WP). Similarly, as for adipocyte differentiation, RFE induced the enrichment of several terms claiming remodelling of the extracellular space, such as *Extracellular matrix organization* ( $P=2.46 \times 10^{-8}$ , REAC), *Collagen formation* ( $P=0.00015$ , REAC), *Collagen biosynthesis and modifying enzymes* ( $P=0.0004$ , REAC) and *Crosslinking of collagen fibrils* ( $P=0.0026$ , REAC).

**A)****B)**

KEGG		REAC		WP	
Term	P value	Term	P value	Term	P value
Metabolic pathways	2.467 e-06	Extracellular matrix organization	2.463 e-8	Cholesterol Biosynthesis	9.396 e-8
HIF-1 signaling pathway	4.617 e-05	Metabolism	3.585 e-06	Cholesterol metabolism (includes both Bloch and Kandutsch-Russell pathways)	2.347 e-7
Glycolysis / Gluconeogenesis	0.0015	Cholesterol biosynthesis	5.181 e-06	Focal Adhesion-PI3K-Akt-mTOR-signaling pathway	0.0330
Biosynthesis of unsaturated fatty acids	0.0027	Metabolism of carbohydrates	8.172 e-05	Glycolysis and Gluconeogenesis	0.0454
Steroid biosynthesis	0.0030	Collagen formation	0.00015		
Fatty acid metabolism	0.0039	Response to elevated platelet cytosolic Ca <sup>2+</sup>	0.0004		
PPAR signaling pathway	0.0099	Collagen biosynthesis and modifying enzymes	0.0004		
Glucagon signaling pathway	0.0154	Platelet degranulation	0.0009		
Axon guidance	0.0198	Crosslinking of collagen fibrils	0.0026		
PI3K-Akt signaling pathway	0.0329	Keratan sulfate degradation	0.0085		

**Figure 6. Pathway enrichment analysis of RFE-stimulated vs. non-stimulated Adipocytes DEGs. A)** Manhattan plot of significantly enriched terms from the DEGs between Adipocyte RFE-stimulated and non-stimulated. Databases used were Kyoto Encyclopedia of Genes and Genomes (KEGG), Reactome (REAC) and WikiPathways (WP). **B)** Table showing the top 10 most regulated terms of each database.

## **Discussion.**

The blackberry has reportedly been linked to interesting properties such as prevention and treatment of metabolic syndrome, support of the digestive and immune system, prevention of inflammatory disorders, cardiovascular diseases and protective effects against gastrointestinal tract cancers [2]. Moreover, the blackberry is used in cosmetics for skin antiaging and hair protection applications, due to its antioxidant and anti-inflammatory properties [3]. Interestingly, although there is increasing evidence that key components of the blackberry exert various functions regarding the adipogenic system, to our knowledge, to date there is no direct testing of a blackberry extract in its impact in fat accumulation and breakdown, or adipocyte differentiation.

In this regard, previous reports did analyze the impact of different components found in the blackberry for adipogenesis and lipolysis. Probably due to the fact that preceding studies did not test full blackberry extracts, but components found in the blackberry or different extracts containing some molecules shared with the blackberry, these findings provide mixed evidence. In this line, although the anthocyanin cyanidin 3-glucoside (C3G), has been described to limit body weight increase in db/db mice [4, 14], it has also been shown to increase lipid droplets and induce preadipocyte differentiation into adipocytes by up-regulating C/EBP $\beta$  via cAMP in 3T3-L1 cells [15], as well as it has been shown to increase the number and size in lipid droplets in the 3T3-L1 cell model [16] and to limit lipolysis [17]. Another well-known component of the blackberry is Ellagic acid (EA). Similar to C3G, there is conflicting evidence for the role of EA in adipogenesis. On the one hand, it has been shown that EA reduces lipid accumulation in 3T3-L1 preadipocytes [18], but on the other hand it has been conversely reported that, again in 3T3-L1 cells, EA reduces lipolysis and does not interfere with adipogenesis [5], or that EA further promotes adipocyte differentiation from 3T3-L1 preadipocytes induced by insulin [19]. With regards to flavonols, among which quercetin and kaempferol are key for the blackberry properties [2], there is accumulating evidence that both reduce the adipogenic process in 3T3-L1 cells [20-22] via repression of the C/EBP $\beta$  and PPAR $\gamma$  programmes [23]. But on the other hand, kaempferol and quercetin are also described to induce the expression of glucose transporters and increase its uptake by the adipocytes [6, 24, 25]. Taken together, previous evidence regarding components of the

blackberry suggests a potential effect of the blackberry on adipogenesis and lipolysis, but leaves open the question regarding the net effect of a full extract of blackberry on adipocyte maturation and lipolysis.

Provided the previous evidence described above, in the present work we sought to shed some light into the adipogenic properties of the blackberry by directly testing the RFE extract on adipocyte differentiation and lipolysis following a well-established protocol with 3T3-L1 preadipocyte system (Figure 2), the most commonly used *in vitro* system for the study of adipogenesis and lipolysis [26]. Graph on Figure 3A shows the measurement of glycerol levels, a direct assessment of lipolysis in cultured adipocytes [27], upon stimulation with RFE, strongly indicating RFE significantly prevents lipolysis in mature adipocytes. In the same line, Figure 3B depicts the measurement of extracted Red Oil O, commonly used for the quantification of adipocyte differentiation [26], showing that RFE significantly increases adipogenesis, an effect also found by fluorescence staining of lipid droplets with Adipored<sup>TM</sup> (Figure 3C). To our knowledge, this is the first direct description of the impact of a blackberry extract in lipolysis and/or adipogenesis, and strongly indicates that it simultaneously facilitates adipogenesis and inhibits lipolysis.

Transcriptomic analysis in Figure 4 provides additional strong evidence that RFE facilitates adipocyte differentiation. In this regard, the PCA plot (Figure 4C) shows a strong clustering over the PC1 (96.77 % of gene variance) due to adipocyte differentiation and RFE further moves all three replicates over the PC1, which is in strong agreement with the heatmap on Figure 4D, showing the expression of the 500 topmost variable genes. Here, two clusters of gene expression, high and low expressed genes, are visually distinguished when comparing preadipocytes to adipocytes, and represents the transcriptomic fingerprint of 3T3-L1 adipocyte differentiation. Interestingly, the impact of RFE is noticeable not only in a set of genes, but it modulates all 500 genes as a whole in the same direction as adipocyte differentiation itself.

In our hands, 3T3-L1 adipocyte differentiation triggered DEGs mainly related to metabolic processes, as detected in the pathway enrichment analysis when comparing our data with the

KEGG, REACTOME and WP databases (Figure 5B). Further supporting the notion that RFE facilitates adipocyte maturation, the functional analysis of adipocyte differentiation was found similar to that of the functional analysis of RFE stimulation of differentiated adipocytes (Figure 5 vs. Figure 6). In addition, it is remarkable that RFE primarily impacted cellular metabolic pathways, and in particular, those that favor a shift from sugar metabolism to lipid synthesis and its accumulation in the mature adipocyte. This could be explained by the modulation of PPAR signaling pathway achieved by RFE (Figure 6B), as PPAR $\gamma$  is known to be the master regulator of adipogenesis, regulating a wide range of genes expressed in developing and mature adipocytes, like those that are involved in insulin sensitivity, lipogenesis and lipolysis [28, 29].

It is worth noting the relevance of the extracellular matrix (ECM) in the functional analysis found in the present work. In this line, it is well-described that the collagen is the main component of the adipose ECM, that it contributes considerably to the non-cell mass and that it is mainly produced by adipocytes [30], so that the mechanical stress induced by production of triglycerides can be mitigated by a strong external skeleton [30]. In agreement, the functional analysis on Figure 5 highlights the importance of ECM remodeling in adipocyte differentiation. When adipocytes were treated with RFE, many terms related to the ECM and collagen were found enriched (Figure 6), which indicates that RFE not only facilitates adipocyte differentiation in relation to metabolism, but that it also facilitates the remodeling of the extracellular component needed for a healthy adipose tissue expansion [30]. In the same line, in pathological situations such as obesity, accumulation of collagen causes fibrosis of adipose tissue increasing its rigidity [31] and cosmetic disorders such as cellulite are characterized by an ECM with enlarged fibrosclerotic strands [32]. Therefore, our findings suggest that RFE increases the subcutaneous adipose tissue but, at the same time, favors the remodeling of the hypodermal extracellular matrix to allow a healthy adipose tissue growth, limiting fibrosis.

## **Conclusion.**

The present work shows, for the first time to our knowledge, that direct stimulation with a blackberry extract (*Rubus fruticosus* fruit extract, RFE) facilitates adipocyte differentiation in the 3T3-L1 cell model. RFE reduced lipolysis, quantified as glycerol measurement, and increased adipogenesis, as found by Red Oil O quantification and fluorescent AdipoRed™ staining. Furthermore, transcriptomic analysis by RNA-Seq revealed that RFE modulates the adipocyte differentiation transcriptomic fingerprint as a whole, including not only adipocyte metabolism, but also extracellular matrix remodeling suggesting, therefore, that RFE may be of great interest for cosmetic treatments related with facial and body volumizing applications.

## **Acknowledgments.**

For its help and participation in the transcriptomic studies, the authors thank the Bioinformatics Platform of the Max Delbrück Center for Molecular Medicine in Berlin, in particular to Altuna Akalin.

## **Conflict of Interest Statement.**

MPA, ER and JB are full-time employees of Provital S.A.U.

## **References**

- 1 Z. Wang, M. Gerstein, and M. Snyder, “RNA-Seq: A revolutionary tool for transcriptomics,” *Nature Reviews Genetics*. 2009, doi: 10.1038/nrg2484.
- 2 V. Kitrytė, A. Narkevičiūtė, L. Tamkutė, M. Syrpas, M. Pukalskienė, and P. R. Venskutonis, “Consecutive high-pressure and enzyme assisted fractionation of blackberry (*Rubus fruticosus* L.) pomace into functional ingredients: Process optimization and product characterization,” *Food Chem.*, vol. 312, no. July 2019, 2020, doi: 10.1016/j.foodchem.2019.126072.
- 3 M. Zia-Ul-Haq, M. Riaz, V. De Feo, H. Z. E. Jaafar, and M. Moga, “*Rubus fruticosus* L.: Constituents, biological activities and health related uses,” *Molecules*. 2014, doi: 10.3390/molecules190810998.
- 4 T. Matsukawa, T. Inaguma, J. Han, M. O. Villareal, and H. Isoda, “Cyanidin-3-

- glucoside derived from black soybeans ameliorate type 2 diabetes through the induction of differentiation of preadipocytes into smaller and insulin-sensitive adipocytes,” *J. Nutr. Biochem.*, 2015, doi: 10.1016/j.jnutbio.2015.03.006.
- 5 L. Cisneros-Zevallos, W. Y. Bang, and C. Delgadillo-Puga, “Ellagic acid and urolithins A and B differentially regulate fat accumulation and inflammation in 3T3-L1 adipocytes while not affecting adipogenesis and insulin sensitivity,” *Int. J. Mol. Sci.*, 2020, doi: 10.3390/ijms21062086.
- 6 X. K. Fang, J. Gao, and D. N. Zhu, “Kaempferol and quercetin isolated from Euonymus alatus improve glucose uptake of 3T3-L1 cells without adipogenesis activity,” *Life Sci.*, 2008, doi: 10.1016/j.lfs.2007.12.021.
- 7 R. Wurmus *et al.*, “PiGx: reproducible genomics analysis pipelines with GNU Guix,” *Gigascience*, vol. 7, no. 12, Dec. 2018, doi: 10.1093/gigascience/giy123.
- 8 A. Dobin *et al.*, “STAR: ultrafast universal RNA-seq aligner,” *Bioinformatics*, vol. 29, no. 1, pp. 15–21, Jan. 2013, doi: 10.1093/bioinformatics/bts635.
- 9 I. Mohorianu, A. Bretman, D. T. Smith, E. K. Fowler, T. Dalmay, and T. Chapman, “Comparison of alternative approaches for analysing multi-level RNA-seq data,” *PLoS One*, 2017, doi: 10.1371/journal.pone.0182694.
- 10 A. Rau, M. Gallopin, G. Celeux, and F. Jaffrézic, “Data-based filtering for replicated high-throughput transcriptome sequencing experiments,” *Bioinformatics*, 2013, doi: 10.1093/bioinformatics/btt350.
- 11 M. D. Robinson, D. J. McCarthy, and G. K. Smyth, “edgeR: A Bioconductor package for differential expression analysis of digital gene expression data,” *Bioinformatics*, 2009, doi: 10.1093/bioinformatics/btp616.
- 12 H. Peterson, L. Kolberg, U. Raudvere, I. Kuzmin, and J. Vilo, “gprofiler2 -- an R package for gene list functional enrichment analysis and namespace conversion toolset g: Profiler,” *F1000Research*, 2020, doi: 10.12688/f1000research.24956.2.
- 13 U. Raudvere *et al.*, “G:Profiler: A web server for functional enrichment analysis and conversions of gene lists (2019 update),” *Nucleic Acids Res.*, 2019, doi: 10.1093/nar/gkz369.
- 14 Y. You *et al.*, “Cyanidin-3-glucoside increases whole body energy metabolism by upregulating brown adipose tissue mitochondrial function,” *Mol. Nutr. Food Res.*, vol.

- 61, no. 11, 2017, doi: 10.1002/mnfr.201700261.
- 15 T. Matsukawa, M. O. Villareal, H. Motojima, and H. Isoda, “Increasing cAMP levels of preadipocytes by cyanidin-3-glucoside treatment induces the formation of beige phenotypes in 3T3-L1 adipocytes,” *J. Nutr. Biochem.*, vol. 40, pp. 77–85, 2017, doi: 10.1016/j.jnutbio.2016.09.018.
  - 16 T. Inaguma, J. Han, and H. Isoda, “Improvement of insulin resistance by Cyanidin 3-glucoside, anthocyanin from black beans through the up-regulation of GLUT4 gene expression,” *BMC Proc.*, vol. 5, p. 21, 2011, doi: 10.1186/1753-6561-5-s8-p21.
  - 17 C. Björk *et al.*, “Effects of selected bioactive food compounds on human white adipocyte function,” *Nutr. Metab.*, vol. 13, no. 1, pp. 1–10, 2016, doi: 10.1186/s12986-016-0064-3.
  - 18 L. Wang *et al.*, “Ellagic acid reduces adipogenesis through inhibition of differentiation-prevention of the induction of rb phosphorylation in 3T3-L1 Adipocytes,” *Evidence-based Complement. Altern. Med.*, vol. 2013, 2013, doi: 10.1155/2013/287534.
  - 19 A. Perera, S. H. Ton, M. Moorthy, and U. D. Palanisamy, “The insulin-sensitising properties of the ellagitannin geraniin and its metabolites from Nephelium lappaceum rind in 3T3-L1 cells,” *Int. J. Food Sci. Nutr.*, vol. 71, no. 8, pp. 940–953, 2020, doi: 10.1080/09637486.2020.1754348.
  - 20 C. R. Bae, Y. K. Park, and Y. S. Cha, “Quercetin-rich onion peel extract suppresses adipogenesis by down-regulating adipogenic transcription factors and gene expression in 3T3-L1 adipocytes,” *J. Sci. Food Agric.*, vol. 94, no. 13, pp. 2655–2660, 2014, doi: 10.1002/jsfa.6604.
  - 21 I. Eseberri *et al.*, “Effects of quercetin metabolites on triglyceride metabolism of 3T3-L1 preadipocytes and mature adipocytes,” *Int. J. Mol. Sci.*, vol. 20, no. 2, 2019, doi: 10.3390/ijms20020264.
  - 22 S. G. Lee, J. S. Parks, and H. W. Kang, “Quercetin, a functional compound of onion peel, remodels white adipocytes to brown-like adipocytes,” *J. Nutr. Biochem.*, 2017, doi: 10.1016/j.jnutbio.2016.12.018.
  - 23 I. Eseberri, J. Miranda, A. Lasa, I. Churruca, and M. P. Portillo, “Doses of quercetin in the range of serum concentrations exert delipidating effects in 3t3-l1 preadipocytes

- by acting on different stages of adipogenesis, but not in mature adipocytes,” *Oxid. Med. Cell. Longev.*, 2015, doi: 10.1155/2015/480943.
- 24 R. Varshney, R. Mishra, N. Das, D. Sircar, and P. Roy, “A comparative analysis of various flavonoids in the regulation of obesity and diabetes: An in vitro and in vivo study,” *J. Funct. Foods*, 2019, doi: 10.1016/j.jff.2019.05.004.
- 25 L. Cui *et al.*, “Chemical composition and glucose uptake effect on 3T3-L1 adipocytes of *Ligustrum lucidum* Ait. flowers,” *Food Sci. Hum. Wellness*, 2020, doi: 10.1016/j.fshw.2020.02.002.
- 26 N. A. Kraus, F. Ehebauer, B. Zapp, B. Rudolphi, B. J. Kraus, and D. Kraus, “Quantitative assessment of adipocyte differentiation in cell culture,” *Adipocyte*, 2016, doi: 10.1080/21623945.2016.1240137.
- 27 M. Schweiger, T. O. Eichmann, U. Taschler, R. Zimmermann, R. Zechner, and A. Lass, “Measurement of lipolysis,” in *Methods in Enzymology*, 2014.
- 28 S. P. Poulos, M. V. Dodson, M. F. Culver, and G. J. Hausman, “The increasingly complex regulation of adipocyte differentiation,” *Exp. Biol. Med.*, vol. 241, no. 5, pp. 449–456, 2016, doi: 10.1177/1535370215619041.
- 29 C. E. Lowe, S. O’Rahilly, and J. J. Rochford, “Adipogenesis at a glance,” *J. Cell Sci.*, vol. 124, no. 16, pp. 2681–2686, 2011, doi: 10.1242/jcs.079699.
- 30 F. J. Ruiz-Ojeda, A. Méndez-Gutiérrez, C. M. Aguilera, and J. Plaza-Díaz, “Extracellular matrix remodeling of adipose tissue in obesity and metabolic diseases,” *International Journal of Molecular Sciences*. 2019, doi: 10.3390/ijms20194888.
- 31 C. Buechler, S. Krautbauer, and K. Eisinger, “Adipose tissue fibrosis,” *World J. Diabetes*, 2015, doi: 10.4239/wjd.v6.i4.548.
- 32 E. Emanuele, P. Minoretti, K. Altabas, E. Gaeta, and V. Altabas, “Adiponectin expression in subcutaneous adipose tissue is reduced in women with cellulite,” *Int. J. Dermatol.*, 2011, doi: 10.1111/j.1365-4632.2010.04713.x.